Discovery of *C*-(1-aryl-cyclohexyl)-methylamines as selective, orally available inhibitors of dipeptidyl peptidase IV

Kenji Namoto, Finton Sirockin, Nils Ostermann, Francois Gessier, Stefanie Flohr, Richard Sedrani, Bernd Gerhartz, Jörg Trappe, Ulrich Hassiepen, Alokesh Duttaroy, Suzie Ferreira, Jon M. Sutton, David E. Clark, Gary Fenton, Mandy Beswick, Daniel K. Baeschlin

PII: S0960-894X(13)01502-3
DOI: http://dx.doi.org/10.1016/j.bmcl.2013.12.118
Reference: BMCL 21226

To appear in: *Bioorganic & Medicinal Chemistry Letters*

Received Date: 4 November 2013
Revised Date: 27 December 2013
Accepted Date: 28 December 2013

Please cite this article as: Namoto, K., Sirockin, F., Ostermann, N., Gessier, F., Flohr, S., Sedrani, R., Gerhartz, B., Trappe, J., Hassiepen, U., Duttaroy, A., Ferreira, S., Sutton, J.M., Clark, D.E., Fenton, G., Beswick, M., Baeschlin, D.K., Discovery of *C*-(1-aryl-cyclohexyl)-methylamines as selective, orally available inhibitors of dipeptidyl peptidase IV, *Bioorganic & Medicinal Chemistry Letters* (2014), doi: http://dx.doi.org/10.1016/j.bmcl.2013.12.118

Discovery of *C*-(1-aryl-cyclohexyl)-methylamines as selective, orally available inhibitors of dipeptidyl peptidase IV.

Author Names. Kenji Namoto[a], Finton Sirockin[a], Nils Ostermann[a], Francois Gessier[a], Stefanie Flohr[a], Richard Sedrani[a], Bernd Gerhartz[a], Jörg Trappe[a], Ulrich Hassiepen[a], Alokesh Duttaroy[b], Suzie Ferreira[b], Jon M. Sutton[c], David E. Clark[c], Gary Fenton[c], Mandy Beswick[c], and Daniel K. Baeschlin[a].

[a]*Novartis Institutes for BioMedical Research, Novartis Campus, Basel, Switzerland*

[b]*Novartis Institutes for BioMedical Research, Cambridge, MA, USA*

[c]*Argenta Discovery 2009 Ltd., Harlow, CM19 5TR, UK*

Corresponding Author. Kenji Namoto (kenji.namoto@novartis.com); phone: +41 61 696 2550; contact address: Fabrikstrasse-16.4.31, Novartis Pharma AG, Postfach, CH-4002, Basel, Switzerland.

Abstract. The successful launches of dipeptidyl peptidase IV (DPP IV) inhibitors as oral anti-diabetics warrant and spur the further quest for additional chemical entities in this promising class of therapeutics. Numerous pharmaceutical companies have pursued their proprietary candidates towards the clinic, resulting in a large body of published chemical structures associated with DPP IV. Herein, we report the discovery of a novel chemotype for DPP IV inhibition based on the *C*-(1-aryl-cyclohexyl)-methylamine scaffold and its optimization to compounds which selectively inhibit DPP IV at low-nM potency and exhibit an excellent oral phamacokinetic profile in the rat.

Keywords. protease inhibition; dipeptidyl peptidase IV; structure-based drug design; enzyme selectivity; pharmacokinetics; *ex vivo* plasma DPP IV inhibition

The worldwide morbidity caused by diabetes mellitus is increasing at an alarming rate due to the aging population in developed countries and the rapid emergence of a middle class in the developing world.[1] Consequently, the pharmaceutical industry has ramped up its R&D efforts to discover novel oral anti-diabetic therapeutics with enhanced safety and efficacy profiles.[2]

Among the notable advances in this field in recent years are the successful launches of Galvus ®,[3] Januvia ®,[4] Nesina ®,[5] Onglyza ®,[6] and Tradjenta ®,[7] all of which belong to a class of drugs called gliptins, or inhibitors of dipeptidyl peptidase IV (DPP IV). DPP IV is a serine protease belonging to the S9 family and involved in proteolytic processing of the gut incretin hormone GLP-1, thereby down-regulating the duration of the hormone's stimulating effect on insulin secretion during and after the ingestion of a meal.[8] Inhibition of DPP IV has been widely heralded as the first novel mode of action to control diabetes in the many years since the introduction of metformin, offering an attractive alternative to treat patients who fail to respond to, or are contraindicated towards, conventional therapies.[9,10] Herein, we describe the discovery of *C*-(1-aryl-cyclohexyl)-methylamine as a novel DPP IV inhibitor scaffold with the potential for development as a once-daily oral therapeutic.

Our quest for a novel, orally efficacious, long-acting DPP IV inhibitor commenced with the HTS hit ***syn*-7aa** (Figure 1, DPP IV IC_{50} 11.9 μM). Its cyclohexyl core geminally substituted with an aminomethyl group and an aromatic ring represents a hitherto unexplored DPP IV inhibitor scaffold.[11] An X-ray co-crystal structure of ***syn*-7aa** with recombinant human DPP IV (Figure 2) revealed that the cyclohexyl core orients the phenyl ring deep into the S1 pocket where it takes the same orientation as observed for the 2,4,5-trifluorophenyl motif of sitagliptin (pdb:2p8s).[12] The basic aminomethyl side chain interacts with the carboxylates of glutamic acids Glu205 and Glu207.[13] The cinnamyl chain is directed further down to the non-prime side of the active site, albeit with lower electron densities in the X-ray structure, suggesting that there is less specific binding in this region. As observed in our previous studies on deazaxanthine-based DPP IV inhibitors,[14] the side chain of Tyr547 was flipped upwards compared to its position in the co-crystal structure of sitagliptin with DPP IV presumably due to the steric bulk of the cyclohexyl core. With a clear structural proof of binding in hand, we embarked on an initial investigation of the structure-activity relationships of this new chemical class.

Figure 1. Vildagliptin, sitagliptin, and *C*-(1-aryl-cyclohexyl)-methylamine HTS hit ***syn*-7aa**.

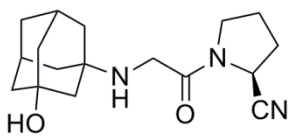

Galvus (vildagliptin),
DPP IV IC_{50} 0.007 μM

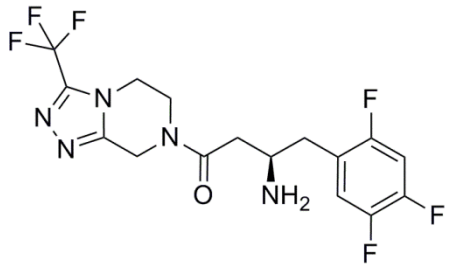

Januvia (sitagliptin),
DPP IV IC_{50} 0.010 μM

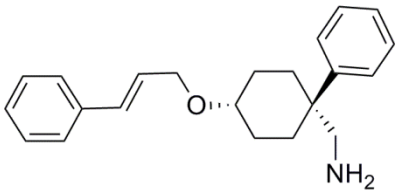

***syn*-7aa**, DPP IV IC_{50} 11.9 μM

Figure 2. An X-ray structure overlay of HTS hit ***syn-7aa*** (ligand shown with ball and stick representation and grey-white carbon atoms, protein in stick representation with grey-white carbon atoms) and Januvia (ligand shown with ball and stick representation and magenta carbon atoms, protein in stick representation with light-pink carbon atoms).

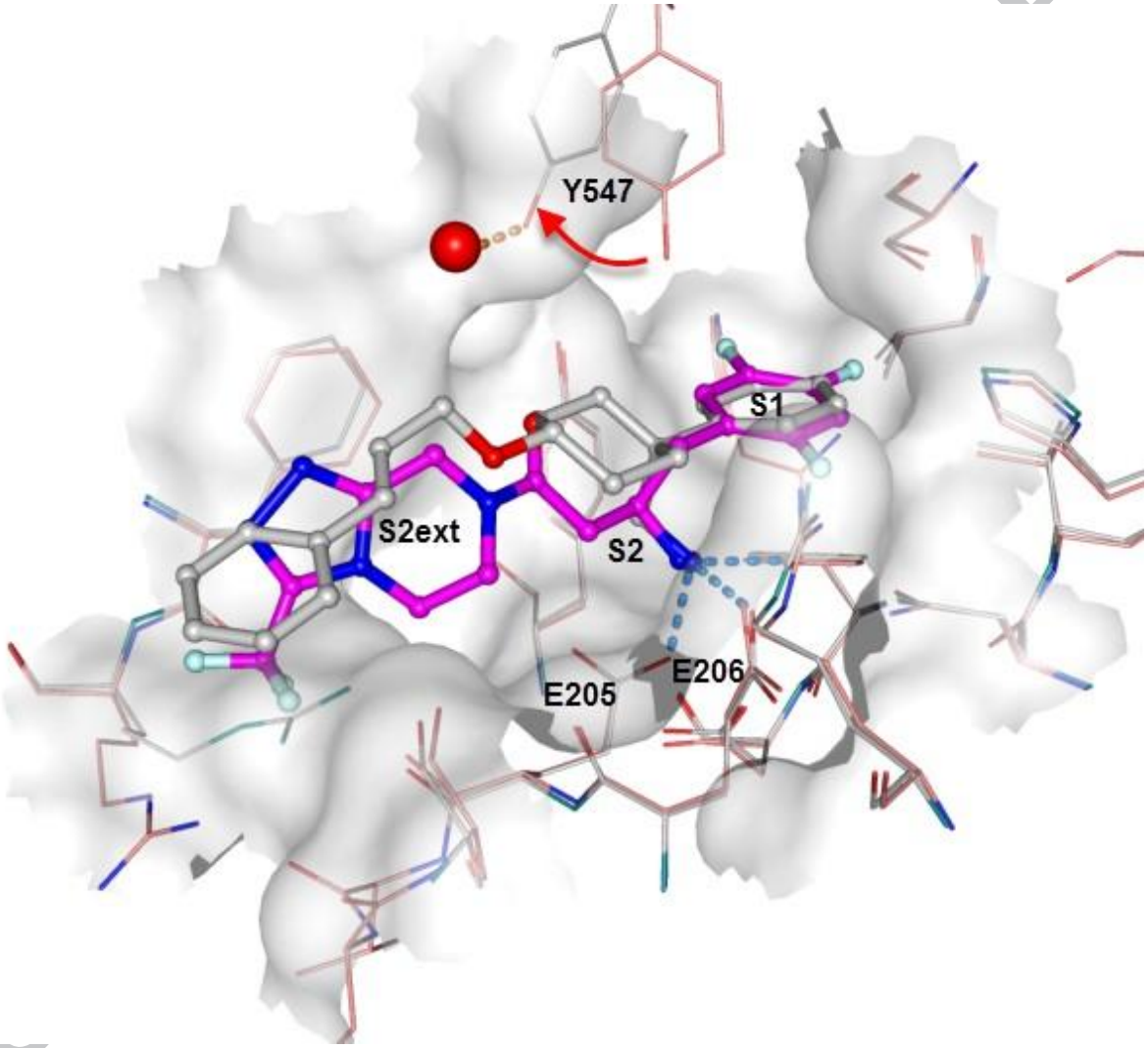

Compounds ***syn*-7aa**–**7c** were prepared according to Scheme 1. Thus, halophenylacetonitriles **1b**–**1c** underwent double Michael addition to methyl acrylate in the presence of Triton B to yield the *bis*-esters **2b**–**2c**, which were cyclized by Dieckmann condensation followed by hydrolytic decarboxylation to afford cyclohexanones **4b**–**4c**.[15] The carbonyl group of cyclohexanones **4a**[16]–**4c** was reduced with sodium borohydride to give the secondary alcohols ***syn*-5a**–**5c** which showed a preference for the *syn* configuration. After chromatographic removal of the minor *anti* stereoisomer, the hydroxyl group of ***syn*-5a**–**5c** was deprotonated and alkylated with alkylhalides, yielding the ethers ***syn*-6aa**–**6c**. Finally, reduction of the nitrile group by borane–THF complex or lithium aluminum hydride gave the cyclohexyl ether derivatives ***syn*-7aa**–**7c**.

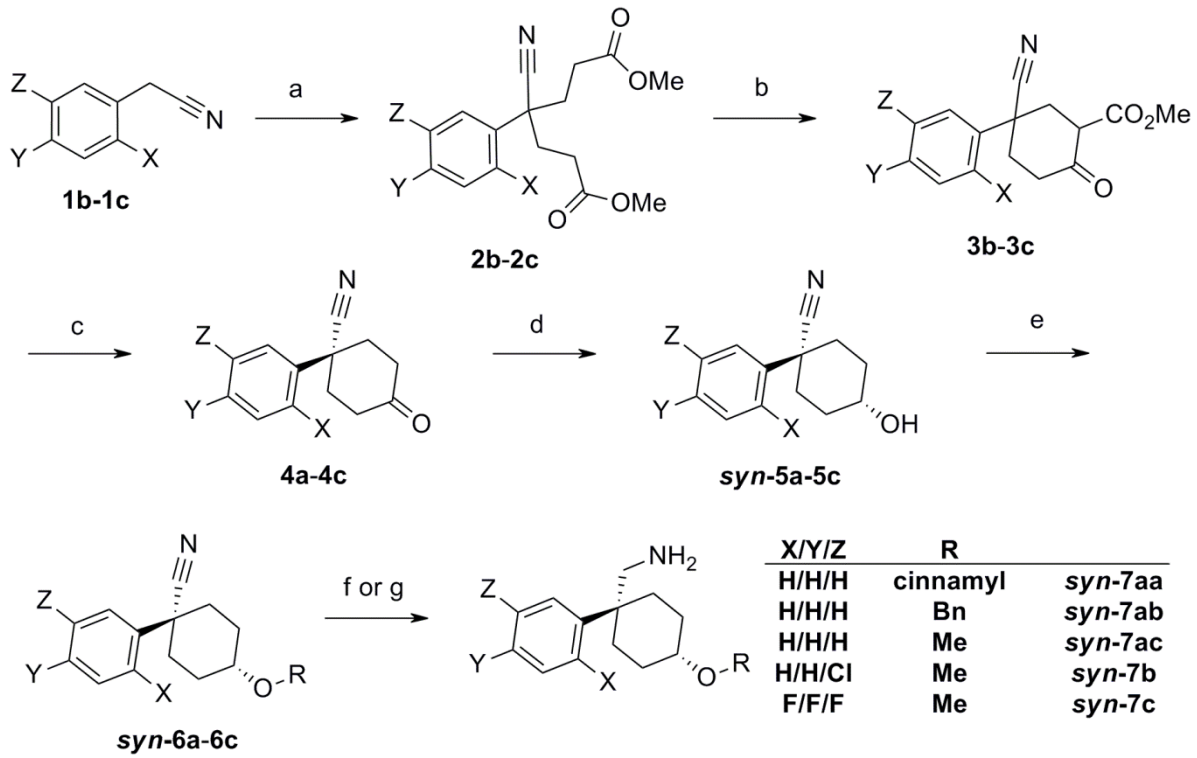

X/Y/Z	R	
H/H/H	cinnamyl	*syn*-7aa
H/H/H	Bn	*syn*-7ab
H/H/H	Me	*syn*-7ac
H/H/Cl	Me	*syn*-7b
F/F/F	Me	*syn*-7c

Scheme 1. Synthesis of cyclohexyl ether derivatives ***syn*-7aa** – **7c**. (a) Methyl acrylate, 40% Triton B in MeOH, *t*-BuOH, reflux, 5h (62-72%); (b) *t*-BuOK, THF, reflux, overnight (40-98%); (c) 10% aq. H_2SO_4 – AcOH [1:2], 110˚C, overnight (42-75%); (d) $NaBH_4$, THF, -78˚C, 1.5h (45-98%);

(e) Alkyl halide RBr or RI, NaH, THF,0˚C then rt, 3h (19-99%); (f) BH_3-THF, THF, reflux, 5h, then 6N aq. HCl, reflux, 2h (7-55%); (g) $LiAlH_4$, THF, 50˚C, 2h (7-24%).

Evaluation of these compounds in a biochemical assay against recombinant human DPP IV quickly revealed two important structure-activity relationships of this chemotype (Table 1),[17] corroborating our observation from the X-ray co-crystal structure. Firstly, truncation of the cinnamyl chain to a benzyl group could be achieved without loss of potency (***syn*-7ab**), indicating a potential for further improvement in activity via additional, more specific, interactions in this region. Further truncation to a methyl group resulted in a six-fold loss of potency but with an improved ligand efficiency of 0.264 (***syn*-7ac**).[18] Secondly, mono-chloro substitution at the meta position of the S1-binding phenyl ring boosted the potency by 15-fold (***syn*-7ac vs *syn*-7b**) while trifluoro substitution, as in sitagliptin, gave only a marginal or low increases in potency (***syn*-7ac vs *syn*-7c**).

Table 1. Biochemical IC_{50} values of ***syn*-7aa** – **7c**.

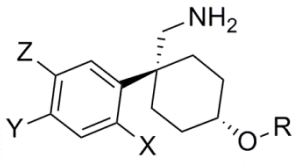

Compounds	X/Y/Z	R	hDPP IV IC_{50} (μM)	Ligand Efficiency
***syn*-7aa**	H/H/H	cinnamyl	11.9	0.205
***syn*-7ab**	H/H/H	Bn	19.9	0.214
***syn*-7ac**	H/H/H	Me	60.0	0.264
***syn*-7b**	H/H/Cl	Me	4.20	0.316
***syn*-7c**	F/F/F	Me	15.7	0.253

In the light of the opportunities identified in the non-prime S2-S3 region to improve the potency further, we closely examined the X-ray co-crystal structures of ***syn*-7aa** and sitagliptin (Figure 2). This led us to the formulation of a three-stage optimization strategy. Firstly, it was envisioned that cyclisation of the flexible cinnamyl ether chain of ***syn*-7aa** should give rise to a better defined overall conformation of the inhibitor, thereby increasing the chance of targeting these P2-P3 moieties towards a specific area of DPP IV S2-S3 region. In particular, fused bicycles

appeared to potentially provide the ideal rigidity and orientation. Secondly, we hypothesized that the "up" conformation of Tyr547 in the ***syn*7aa** structure would allow a unique opportunity for a water-mediated interaction, bridging a hydrogen bond between the ligand and the Tyr547 side-chain hydroxyl group. The distance between the crystallographic water oxygen and the Tyr547 side-chain hydroxyl oxygen is 2.6 Å, showing that this water molecule is clearly hydrogen bonded with Tyr547. Thirdly, and building further upon the two strategies above, we removed the second ring of the fused bicycle and appended it under the first ring, based on an overlay of X-Ray structures of ***syn-7aa*** and sitagliptin (*cf.*Figure 2). This virtual molecule and other putative ligands were manually built into the ***syn-7aa*** X-ray structure and subjected to minimisation with the OPLS force-field (MacroModel 9.0, Schrödinger, Inc.). Different rings were modelled to attach to the cyclohexane present in ***syn-7aa*** replacing the ether moiety and focusing on designing a molecule with a substitution allowing for interaction with the water molecule discussed above. This process eventually resulted in a modified ***syn-7aa*** bearing a pyridazinone ring directly linked to the central cyclohexane.

With this structure-based rationale in mind, we designed and synthesized heterobicyclic derivatives **12a**-**c** and **13a**-**c**, according to Scheme 2, while pyridazinone derivatives **20a**-**d** were prepared according to Scheme 3. Thus, the nitrile and keto carbonyl groups of intermediate **4c** were simultaneously reduced and Boc-protected to give rise stereoselectively to the *syn*-Boc-aminomethylcyclohxanol **8**, which then underwent a two-step Mitsunobu inversion protocol, providing the anti-Boc-aminomethylcyclohexanol **9**. The hydroxyl group was converted to the mesylate, then to the azide, which was reduced to install an amino group with the opposite stereochemistry. Acylation of the primary amine **10** with 5-chlorovaleryl chloride followed by intramolecular cyclisation with sodium hydride furnished the lactam **11**. Boc removal gave compound **12a** and subsequent reduction of the lactam carbonyl yielded compound **13a**. In parallel, the ketone of intermediate **4c** was protected with 1,3-dioxolane, and the nitrile was reduced with lithium aluminum hydride to afford the primary amine **14**, which was subsequently

protected with a Boc group and treated with pyridine-*p*TsOH complex in aqueous media to reveal the ketone **15** chemoselectively. Reductive amination of the ketone carbonyl group with heterobicycle **16** furnished the intermediate **17**, which underwent RuO_2-catalyzed benzylic oxidation and Boc removal to yield compounds **12b-c**,[19] while direct amine deprotection of **17** gave rise to the corresponding deoxo-derivatives **13b-c**. Finally, compounds **20a-d** were prepared in two synthetic steps from the *anti* cyclohexanol **9** using Mitsunobu chemistry with the corresponding pyridazinones **18a-d** and Boc removal of the desired *syn* stereoisomers **19a-d** with TFA in DCM (Scheme 3).[20]

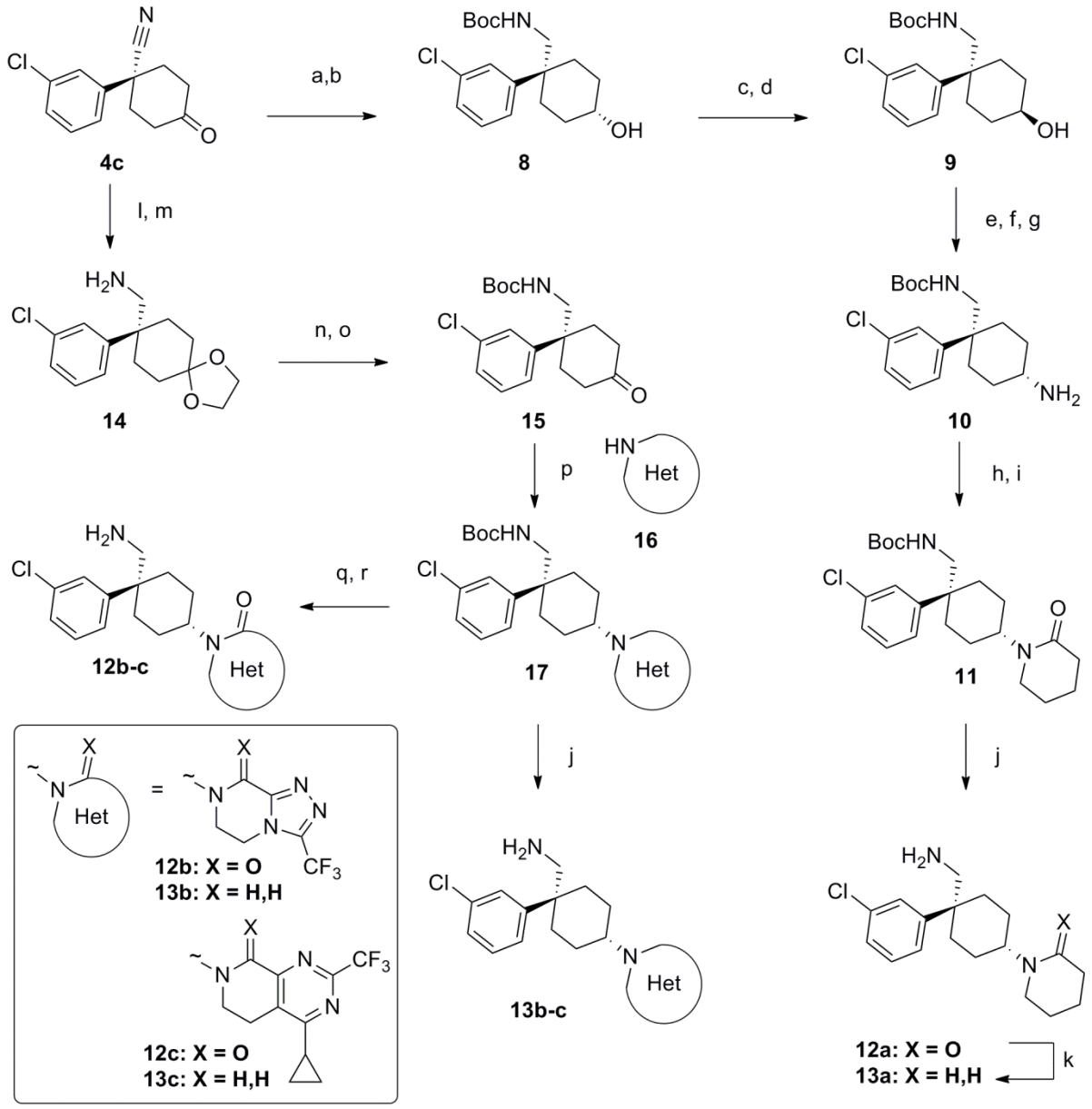

Scheme 2. Synthesis of heterobicyclic derivatives **12a-c** and **13a-c**. (a) BH_3-THF, THF, reflux, 4h, then 2N aq. HCl, r.t. 16h (quant.) (b) Boc_2O, TEA, THF, r.t. 16h (87%) (c) Benzoic acid, PPh_3, DIAD, THF, r.t. 20h (63%) (d) NaOMe, MeOH, THF, r.t. 15h (92%); (e) MsCl, TEA, DCM, r.t. 2h (94%); (f) NaN_3, DMF, 100˚C, 5h (97%) (g) PPh_3, H_2O, toluene, 50˚C, 20h (77%); (h) 5-Chlorovaleryl chloride, sat. aq. Na_2CO_3, $CHCl_3$, r.t. 45min (quant.); (i) NaH, DMF, r.t. 16h (77%); (j) TFA, DCM, r.t. 1h (72-92%); (k) BH_3-THF, THF, reflux, 2d, then 1N aq. HCl, MeOH, 90˚C, 7h

(37%); (l) Ethylene glycol, pTSA, toluene, reflux, 18h (89%); (m) $LiAlH_4$, THF, r.t. 1h then 50˚C, 2h (93%); (n) Boc_2O, TEA, DCM, r.t. 4h (quant.) (o), PPTS, acetone, H_2O, reflux, 2d (50%); (p) $NaBH(OAc)_3$, heterobicycle **16**, AcOH, 1,2-DCE, r.t. 5h (10-50%); (q) $RuO_2 \cdot 2H_2O$, $NaIO_4$, $CHCl_3$, MeCN, H_2O, r.t. 20min (19-76%); (r) TFA, DCM, r.t. 1h (61% for **12b**) or 4N HCl in dioxane, r.t. 2.5h (67% for **12c**).

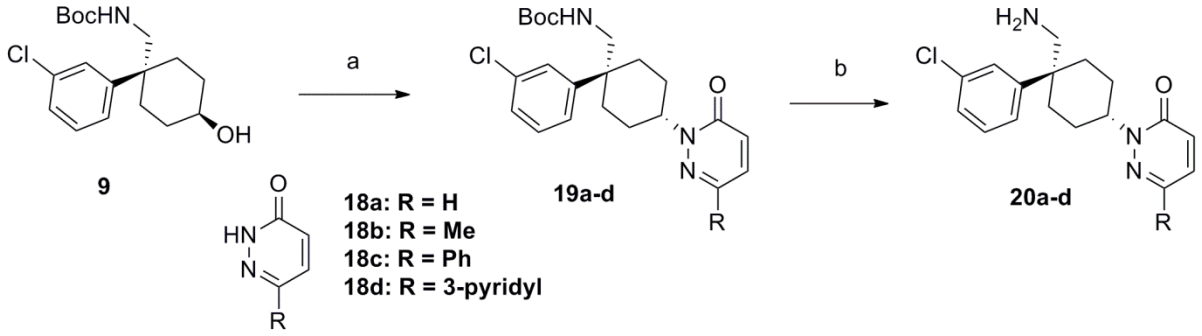

Scheme 3. Synthesis of pyrdidazinone derivatives **20a-d**. (a) DEAD, polymer-supported PPh_3, pyridazinone **18**, THF, r.t. 24h (15-60%); (b) TFA, DCM, r.t. 1h (28-95%).

Evaluation of the compounds thus obtained (Table 2) in the primary assay revealed that all of them were significantly more potent than the acyclic compounds (*cf.* Table 1). In addition, potency enhancements of 5- to 13-fold were observed for the lactam derivatives **12a-c** carrying P2-P3 motifs A, B, and C (X = O) compared with the corresponding de-oxo homologs **13a-c** (X = H,H). We surmised that the lactam group endowed compounds **12a-c** with a higher rigidity of the respective ring systems as well as an additional H-bonding interaction with Tyr547. An X-ray structure of **12a** in complex with human DPP IV revealed that the P1-P2 moieties of the molecules were perfectly aligned with the initial structure of ***syn*-7aa**.[21] Furthermore, this structure unequivocally proved that the designed interaction between the piperidinone carbonyl and a water molecule bridging a hydrogen bond to Tyr547 side-chain hydroxyl was indeed present (Figure 3). Gratifyingly, the pyridazinone compounds **20c-d** were as potent as the bicyclic lactam compounds **12b-c**, validating the original modelling hypothesis for isosteric replacement of the heterobicycle with the heterobiaryl moiety. The selectivity window over the closely related S9 family members DPP8 and 9 improved as the size of the P2-P3 motifs increased from monocycles (60- to 750-fold, **12a**, **13a**, **20a**-**b**) to bicycles (750- to 3700-fold, **12b-c**, **13b-c**) or biaryls (6500- to 8200-fold, **20c-d**).[22]

Table 2. Biochemical IC_{50} values of **12a**-**c**, **13a**-**c**, **20a**-**d**, and sitagliptin.

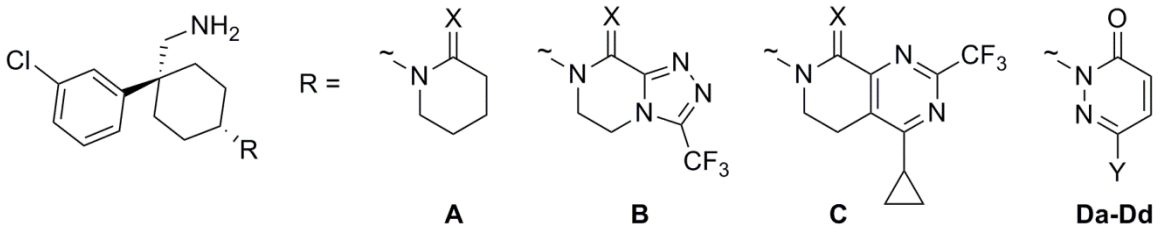

Compounds	R	X	Y	hDPP IV IC_{50} (μM)	Ligand Efficiency	hDPP8 IC_{50} (μM)	hDPP9 IC_{50} (μM)
12a	A	O	-	0.020	0.350	10.8	9
12b	B	O	-	0.007	0.281	22.4	13
12c	C	O	-	0.002	0.264	7.4	3.5
13a	A	H,H	-	0.250	0.314	14.7	14.6
13b	B	H,H	-	0.040	0.264	30	>30
13c	C	H,H	-	0.009	0.251	>30	>30
20a	Da	-	H	0.200	0.305	NT	17.6
20b	Db	-	Me	0.040	0.322	28.3	>30
20c	Dc	-	Phenyl	0.003	0.304	19.4	24.6
20d	Dd	-	3-pyridyl	0.004	0.300	>30	>30
sitagliptin	-	-	-	0.010	0.286	32.8	61.9

Figure 3. An X-ray structure of compound **12a** (ligand shown with ball and stick representation and orange carbon atoms, protein in stick representation with grey-white carbon atoms).

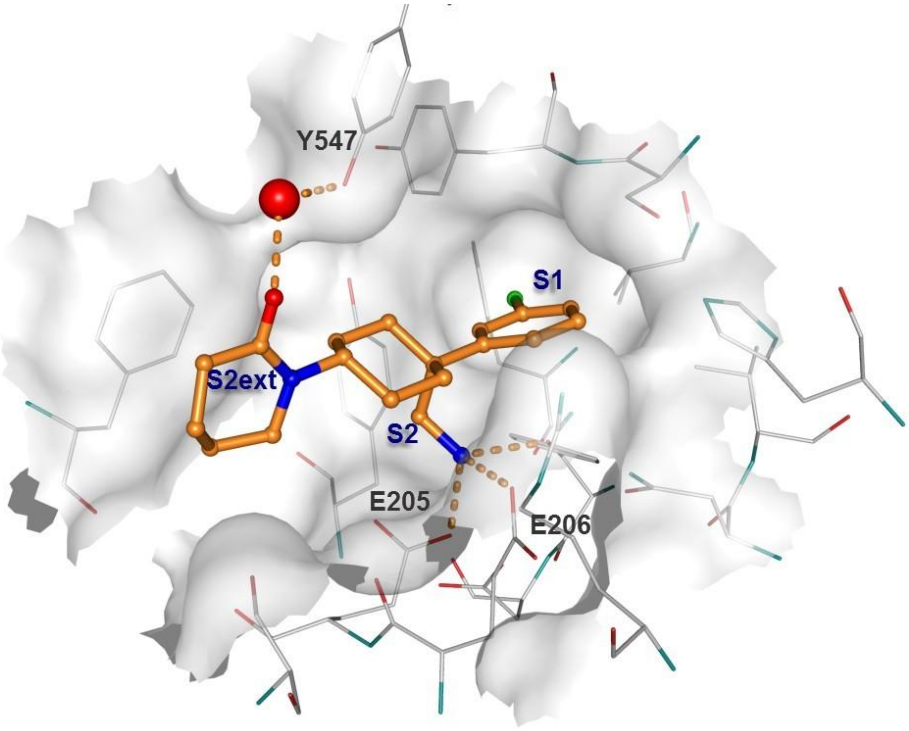

Three compounds with the best potency and selectivity windows **12b**, **12c**, and **20d** were chosen for further evaluation in *in vitro* ADMET assays and pharmacokinetic studies in the rat (Table 3). There appeared to be an *in-vitro* / *in-vivo* disconnect in clearance for **12b**, **12c**, and **20d** which cannot be easily explained. However, oral bioavailability (F_{oral}) followed CaCo-2 permeability well. Compound **12b** exhibited relatively low Caco-2 permeability with moderate clearance in rat microsomes and high *in vivo* clearance, suggesting some extrahepatic clearance. Consequently, the overall exposure was low albeit a measurable oral bioavailability of 17%. Compound **12c**, on the other hand, had a moderate microsomal clearance but enjoyed the lowest *in vivo* clearance among the three compounds. Helped by higher permeability, it achieved a very good oral exposure and a high C_{max} with an admirable 78% bioavailability. Finally, compound **20d** was found to be highly permeable in the Caco-2 assay, which translated well into the *in vivo* setting, with this compound achieving an excellent oral bioavailability of 92%. However, the overall exposure of **20d** was slightly less than that of compound **12c** due to its moderate *in vivo* clearance. Compared with the other two compounds (**12b** and **12c**), **20d** exhibited improved CYP2D6 profile, indicative of a reduced DDI potential, although the prospect of hERG-mediated cardiotoxicity still remains a possibility.

Table 3. Selected ADMET and rat PK data for Compounds **12b**, **12c**, and **20d**.

Compounds	Caco-2 AB/BA (10^{-6} cm/sec)	Rat CL_{int} [a] (μL/min/mg)	CYP2D6 IC_{50} (μM)	hERG [b] IC_{50} (μM)
12b	1.6/4.8	21.9	4.5	>30
12c	4.4/11	43.4	10	0.26
20d	8.6/13	51.1	>10	4.4

[a] rat liver microsome data (RLM). [b] Dofetilide binding assay.

Compounds	T_{max} [c] (h)	C_{max} [c] (nM)	AUC p.o. $_{(0\text{-}8\ h)}$ [c] (nM*h)	Vss [d] (L/Kg)	$T_{1/2}$ [d] (h)	CL [d] (mL/min/kg)	F_{oral} [c] (%)
12b[e]	3.3	57.8	214	11.7	2.7	69	17
12c[f]	3.3	1900	7908	2.1	2.3	9.5	78
20d[g]	1.8	921	4009	3.9	2.2	29	92

[c] *p.o.* leg run at 3 mg/kg. [d] *i.v.*leg run at 1 mg/kg. [e] solution in PBS buffer pH 6.88. [f] solution in sodium acetate buffer pH 4.63. [g] solution in 10% PEG300 / 90% PBS.

Compound **20d** was further assessed, together with sitagliptin, in our rat PD model using *ex vivo* plasma DPP IV inhibition as the pharmacological readout (Figure 4). The compounds were orally administered at 3mg/kg dose, and the DPP IV activity in plasma was monitored over an eight-hour period. Sitagliptin reached a peak inhibition level of 82% at around one to two hours post dose, and then steadily lost its inhibitory activity over the time-course ending in 30% DPP IV inhibition at eight hours post dose. On the other hand, compound **20d** exhibited a superior profile, achieving both a faster onset of half an hour and a higher peak inhibition of 91%, which was maintained at nearly 80% at the end of the eight-hour time-course. The overall *ex vivo* plasma DPPIV inhibition profile of **20d** correlated well with its plasma exposure levels (the exposure data not shown). The excellent duration of action for **20d** clearly demonstrates the potential for this class of DPP IV inhibitors for development as once-daily oral therapeutics.

Figure 4. Inhibition of plasma DPP IV activity after oral administration of compound **20d** and sitagliptin (both at 3 mg/kg dose) in SD rats.

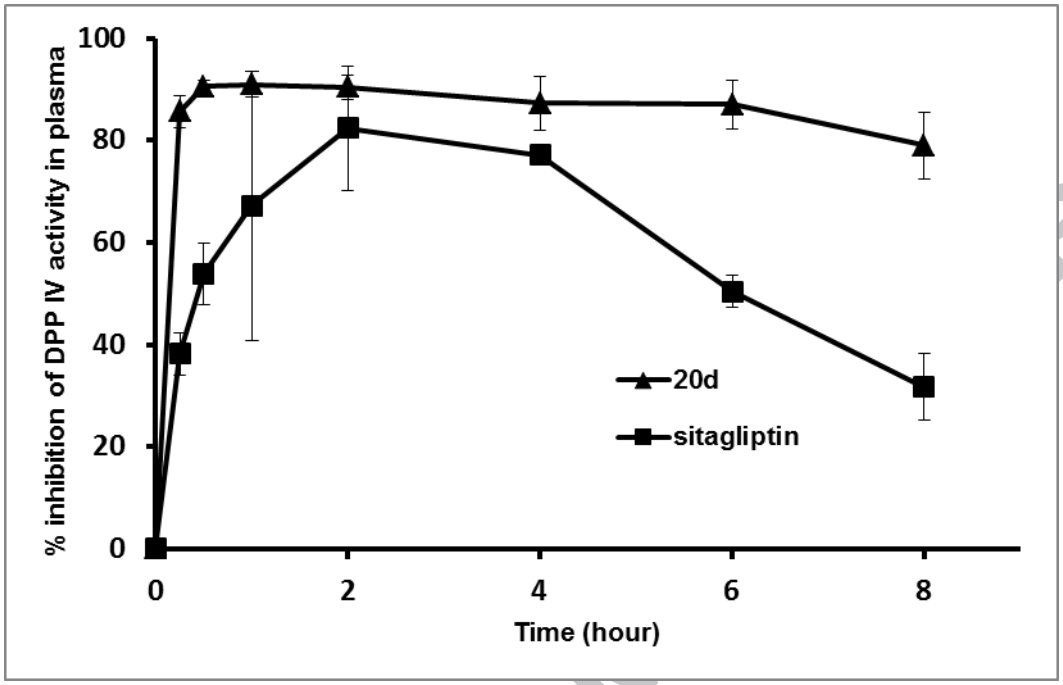

In conclusion, we have discovered a hitherto unexplored class of DPP IV inhibitors featuring the *C*-(1-aryl-cyclohexyl)-methylamine scaffold. Structure-guided medicinal chemistry efforts on the original screening hit ***syn*-7aa** led to successful improvement of target potency in this novel chemotype, resulting in a number of potent, selective and orally bioavailable DPP IV inhibitors. The most advanced derivative, **20d**, demonstrated significantly enhanced duration of DPP IV inhibition in the rat compared with the marketed drug sitagliptin, warranting further endeavour in this arena towards safe and orally efficacious, once-daily antidiabetics.

Acknowledgement

The authors thank Florence Zink for her excellent technical assistance in protein crystallization and Xia Zhang for running *ex vivo* plasma DPP IV assay (Novartis Institutes for BioMedical Research). Numerous contributions to medicinal and synthetic chemistry in this work from the

following individuals at Argenta Disovery are greatly acknowledged: Amanda Fillmore, Neil Harris, Fabien Roussel, Guilaume Brandt, Paul Bury, Rachel Ord and Gwen Hicken.

References

1. Danaei, G.; Finucane, M. M.; Lu, Y.; Singh, G. M.; Cowan, M. J.; Paciorek, C. J.; Lin, J. K.; Farzadfar, F.; Khang, Y.-H.; Stevens, G. A.; Rao, M.; Ali, M. K.; Riley, L. M.; Robinson, C. A.; Ezzati, M. Lancet 2011, 378(9785), 31.

2. “The Pharmaceutical Industry And Global Health – Facts And Figures 2012” International Federation of Pharmaceutical Manufacturers & Associations (2013).

3. Hedge, S.; Schmidt, M. Annu. Rep. Med. Chem. 2008, 43, 494, and references therein.

4. Hedge, S.; Schmidt, M. Annu. Rep. Med. Chem. 2007, 42, 541, and references therein.

5. Bronson, J.; Dhar, M.; Ewing, W.; Lonberg, N. Annu. Rep. Med. Chem. 2011, 46, 446, and references therein.

6. Hedge, S.; Schmidt, M. Annu. Rep. Med. Chem. 2010, 45, 521, and references therein.

7. Bronson, J.; Dhar, M.; Ewing, W.; Lonberg, N. Annu. Rep. Med. Chem. 2012, 47, 540, and references therein.

8. Mentlein, R.; Gallwitz, B.; Schmidt, W.E. Eur. J. Biohem. 1993, 214(3), 829.

9. Barnett, A. Int. J. Clin. Pract. 2006, 60(11), 1454.

10. Deacon, C. F.; Holst, J. Expert Opin. Pharmacother. 2013, 14(15), 2047.

11. To the best of our knowledge, the only related compound known in the literature is a singleton DPP IV inhibitor (human DPP IV IC50 30 µmol) reported in: Nordhoff, S.; Cerezo-Gálvez, S.; Feurer, A.; Hill, O.; Matassa, V. G.; Metz, G.; Rummey, C.; Thiemann, M.; Edwards, P. J. Bioorg. Med. Chem. Lett. 2006, 16, 1744.

12. Biftu, T.; Scapin, G.; Singh, S.; Feng, D.; Becker, J.W.; Eiermann, G.; He, H.; Lyons, K.; Patel, S.; Petrov, A.; Sinha-Roy, R.; Zhang, B.; Wu, J.; Zhang, X.; Doss, G.A.; Thornberry, N.A.; Weber, A.E. Bioorg. Med. Chem. Lett. 2007, 17, 3384.

13. The structure is deposited in the RCSB Protein Data Bank (http://www.rcsb.org/pdb/home/home.do). PDB ID: 4N8D.

14. Sutton, J.M.; Clark, D.E.; Dunsdon, S.J.; Fenton G.; Fillmore, A.; Harris, N.V.; Higgs C.; Hurley, C.A.; Krintel, S.L.; MacKenzie, R.E.; Duttaroy, A.; Gangl, E.; Maniara, W.; Sedrani, R.; Namoto, K.; Ostermann, N.; Gerhartz, B.; Sirockin, F.; Trappe, J.; Hassiepen, U.; Baeschlin, D.K. Bioorg. Med. Chem. Lett. 2012, 22, 1464.

15. Uyeo, S; Shirai, H.; Koshiro, A.; Yashiro, T.; Kagei, K.; Chem. Pharm. Bull. 1966, 14 (9), 1033.

16. Cyclohexane 4a was purchased from Acros Organics (Belgium).

17. DPP IV assays were performed as described in: Sutton, J.M.; Clark, D.E.; Dunsdon, S.J.; Fenton G.; Fillmore, A.; Harris, N.V.; Higgs C.; Hurley, C.A.; Krintel, S.L.; MacKenzie, R.E.; Duttaroy, A.; Gangl, E.; Maniara, W.; Sedrani, R.; Namoto, K.; Ostermann, N.; Gerhartz, B.; Sirockin, F.; Trappe, J.; Hassiepen, U.; Baeschlin, D.K. Bioorg. Med. Chem. Lett. 2012, 22, 1464.

18. Hopkins, A. L.; Groom, C. R.; Alex, A. Drug Discovery Today 2004, 9, 430.

19. Tanaka, K.; Yoshifuji, S.; Nitta, Y. Chem. Pharm. Bull. 1988, 36, 3125.

20. Kuroda, S.; Takamura, F.; Tenda, Y.; Itani, H.; Tomishima, Y.; Akahane, A.; Sakane, K. Chem. Pharm. Bull. 2001, 49, 988.

21. The structure is deposited in the RCSB Protein Data Bank (http://www.rcsb.org/pdb/home/home.do). PDB ID: 4N8E.

22. DPP8/9 assays were performed as described in: Burkey, B. F.; Hoffmann, P. K.; Hassiepen, U.; Trappe, J.; Juedes, M.; Foley, J. E. Diabetes, Obesity and Metabolism 2008, 8, 1057.

Table 1. Biochemical IC_{50} values of ***syn*-7aa** – **7c**.

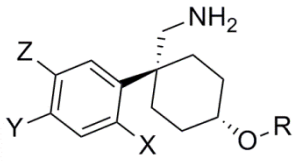

Compounds	X/Y/Z	R	hDPP IV IC_{50} (μM)	Ligand Efficiency
***syn*-7aa**	H/H/H	cinnamyl	11.9	0.205
***syn*-7ab**	H/H/H	Bn	19.9	0.214
***syn*-7ac**	H/H/H	Me	60.0	0.264
***syn*-7b**	H/H/Cl	Me	4.20	0.316
***syn*-7c**	F/F/F	Me	15.7	0.253

Table 2. Biochemical IC_{50} values of **12a**-**c**, **13a**-**c**, **20a**-**d**, and sitagliptin.

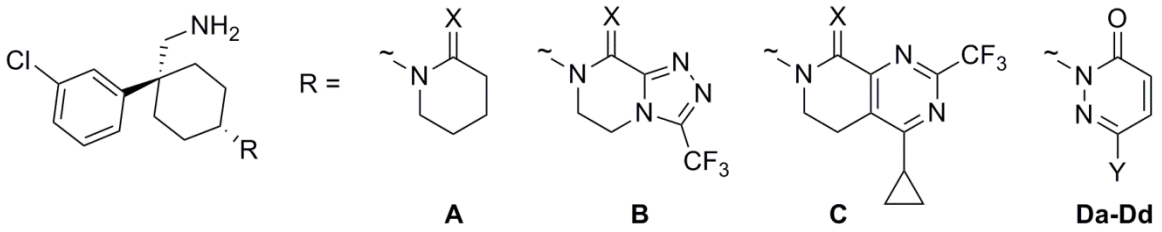

Compounds	R	X	Y	hDPP IV IC_{50} (μM)	Ligand Efficiency	hDPP8 IC_{50} (μM)	hDPP9 IC_{50} (μM)
12a	A	O	-	0.020	0.350	10.8	9
12b	B	O	-	0.007	0.281	22.4	13
12c	C	O	-	0.002	0.264	7.4	3.5
13a	A	H,H	-	0.250	0.314	14.7	14.6
13b	B	H,H	-	0.040	0.264	30	>30
13c	C	H,H	-	0.009	0.251	>30	>30
20a	Da	-	H	0.200	0.305	NT	17.6
20b	Db	-	Me	0.040	0.322	28.3	>30
20c	Dc	-	Phenyl	0.003	0.304	19.4	24.6
20d	Dd	-	3-pyridyl	0.004	0.300	>30	>30
sitagliptin	-	-	-	0.010	0.286	32.8	61.9

Table 3. Selected ADMET and rat PK data for Compounds **12b**, **12c**, and **20d**.

Compounds	Caco-2 AB/BA (10^{-6} cm/sec)	Rat CL_{int} [a] (μL/min/mg)	CYP2D6 IC_{50} (μM)	hERG [b] IC_{50} (μM)
12b	1.6/4.8	21.9	4.5	>30
12c	4.4/11	43.4	10	0.26
20d	8.6/13	51.1	>10	4.4

[a] rat liver microsome data (RLM). [b] Dofetilide binding assay.

Compounds	T_{max} [c] (h)	C_{max} [c] (nM)	AUC p.o. $_{(0\text{-}8\ h)}$ [c] (nM*h)	Vss [d] (L/Kg)	$T_{1/2}$ [d] (h)	CL [d] (mL/min/kg)	F_{oral} [c] (%)
12b[e]	3.3	57.8	214	11.7	2.7	69	17
12c[f]	3.3	1900	7908	2.1	2.3	9.5	78
20d[g]	1.8	921	4009	3.9	2.2	29	92

[c] *p.o.* leg run at 3 mg/kg. [d] *i.v.*leg run at 1 mg/kg. [e] solution in PBS buffer pH 6.88. [f] solution in sodium acetate buffer pH 4.63. [g] solution in 10% PEG300 / 90% PBS.

Figure1

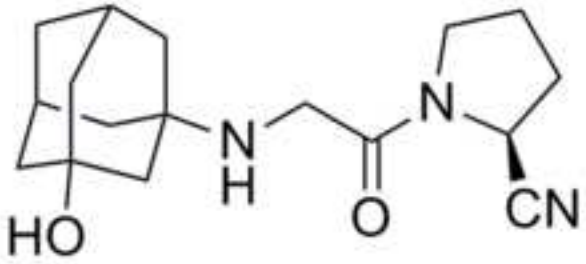

Galvus (vildagliptin),
DPP IV IC_{50} 0.007 μM

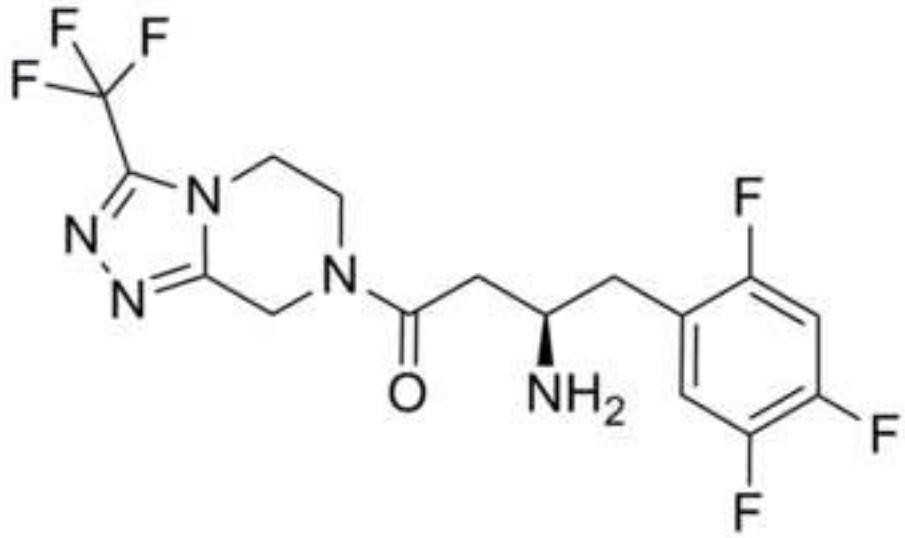

Januvia (sitagliptin),
DPP IV IC_{50} 0.010 μM

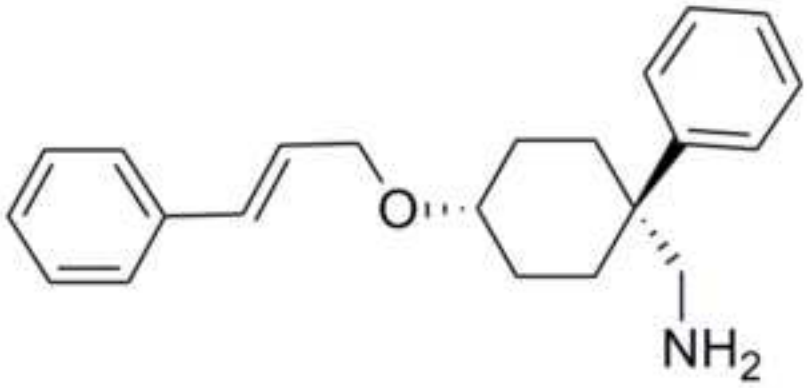

***syn*-7aa**, DPP IV IC_{50} 11.9 μM

Figure2_Color_Web_and_Print

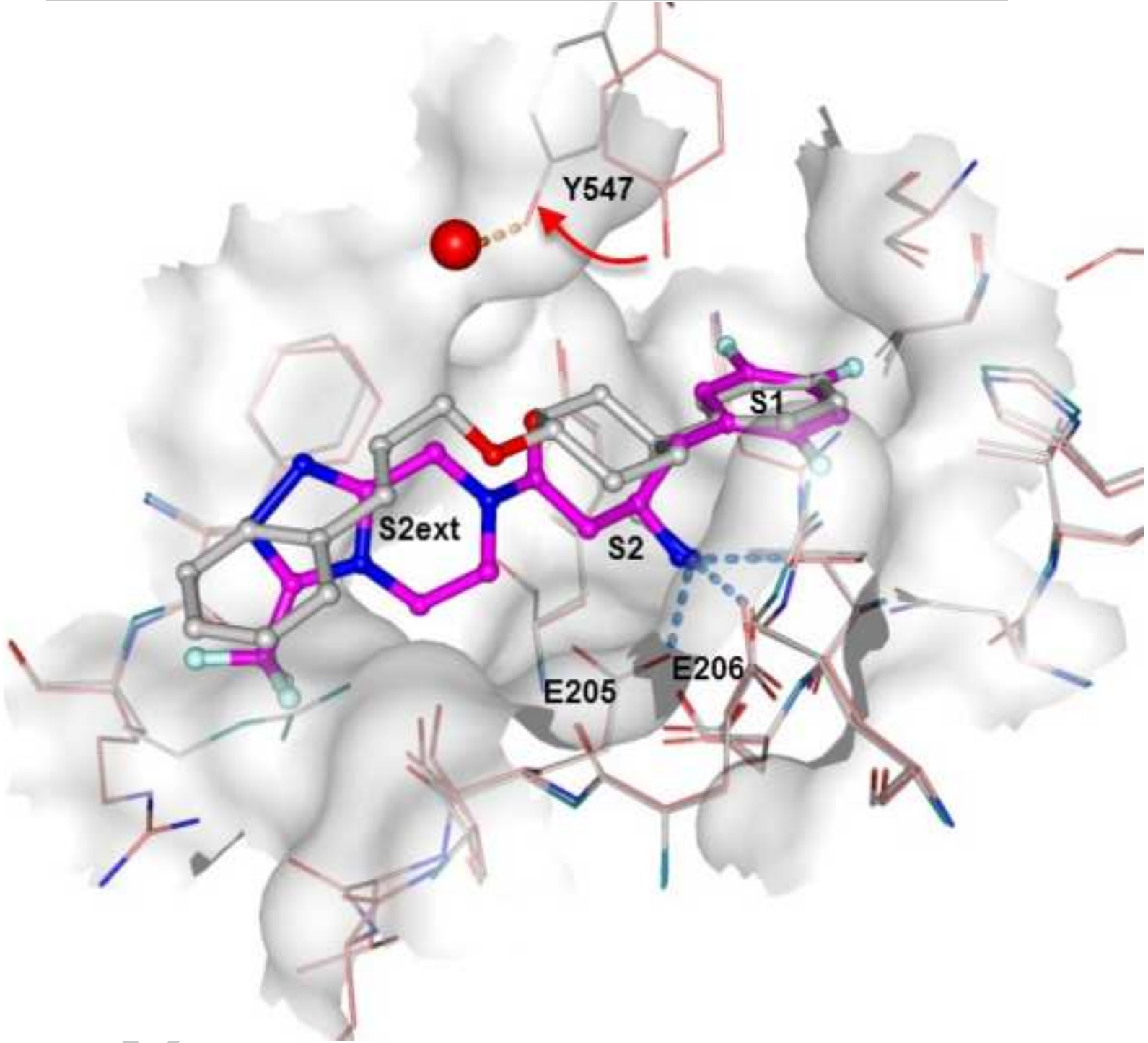

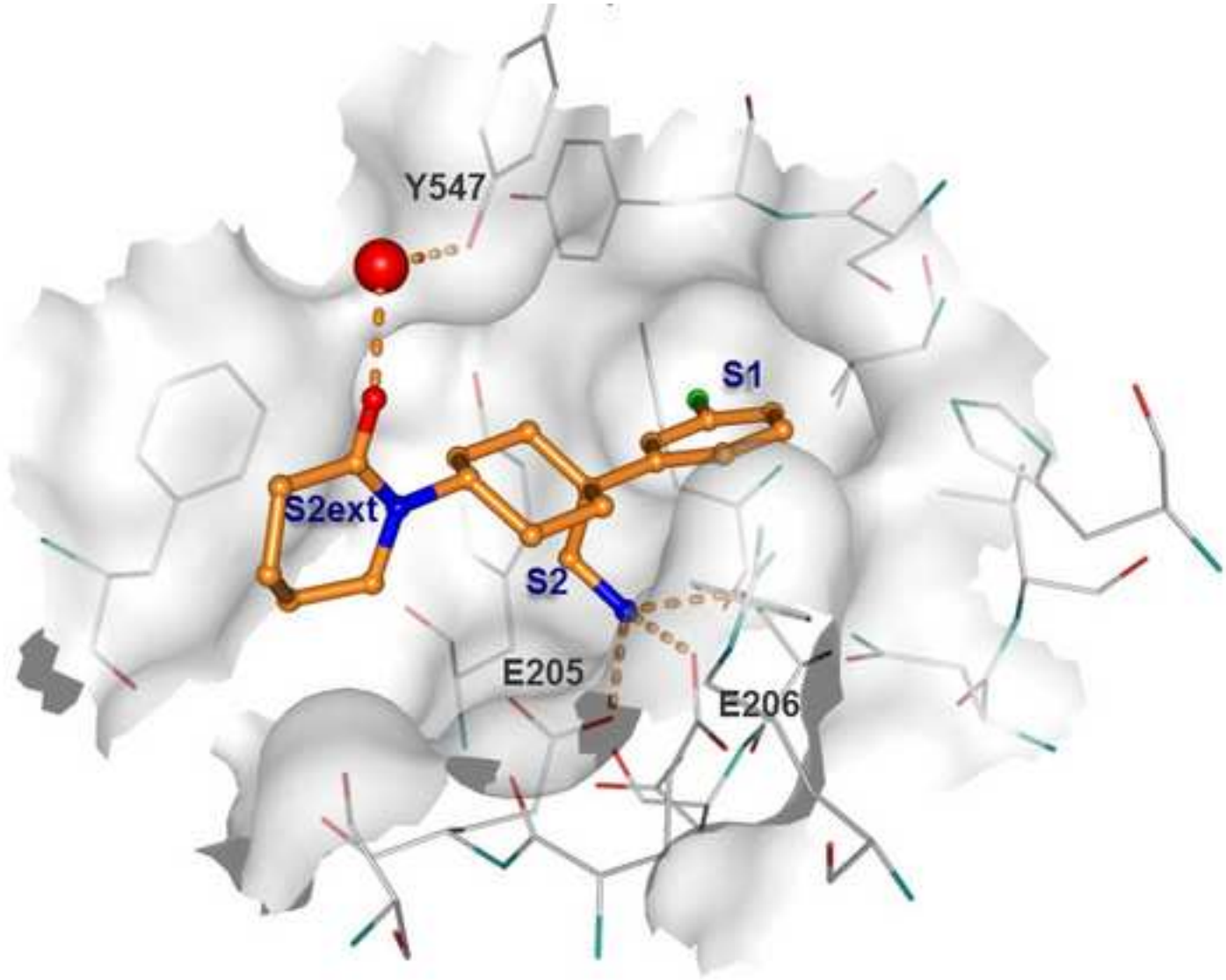

Figure4

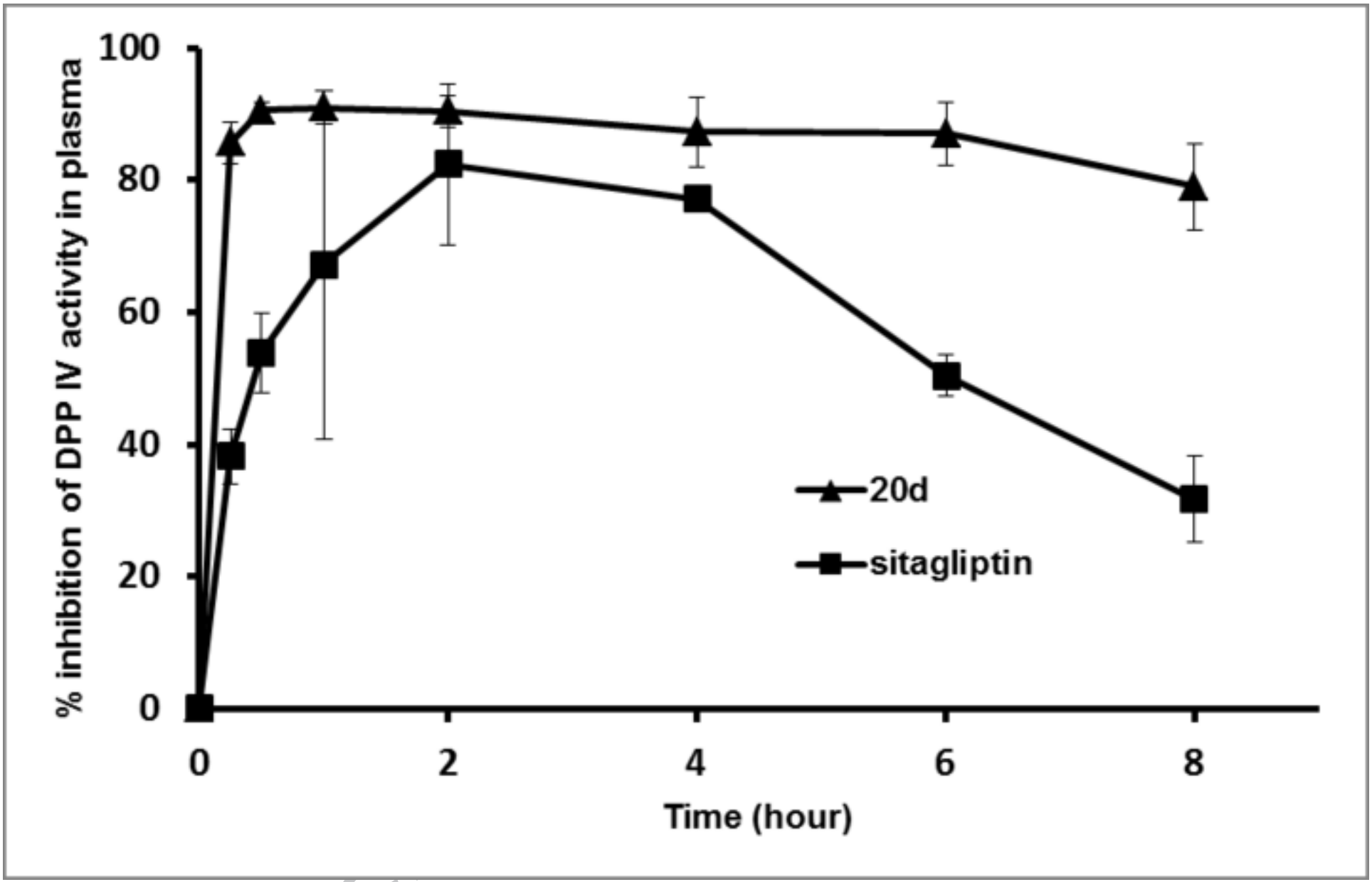

Scheme1

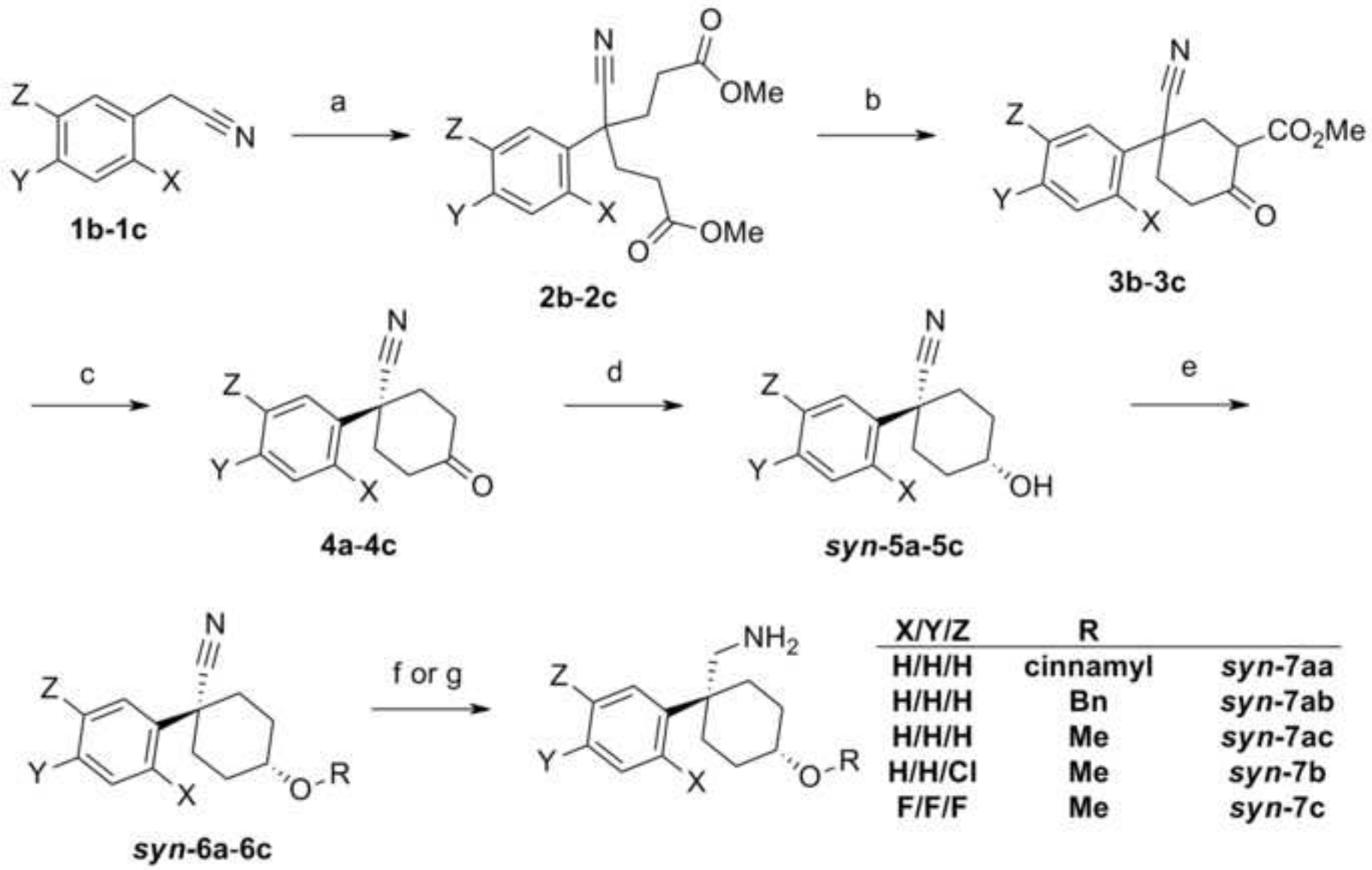

X/Y/Z	R	
H/H/H	cinnamyl	*syn*-7aa
H/H/H	Bn	*syn*-7ab
H/H/H	Me	*syn*-7ac
H/H/Cl	Me	*syn*-7b
F/F/F	Me	*syn*-7c

Scheme2

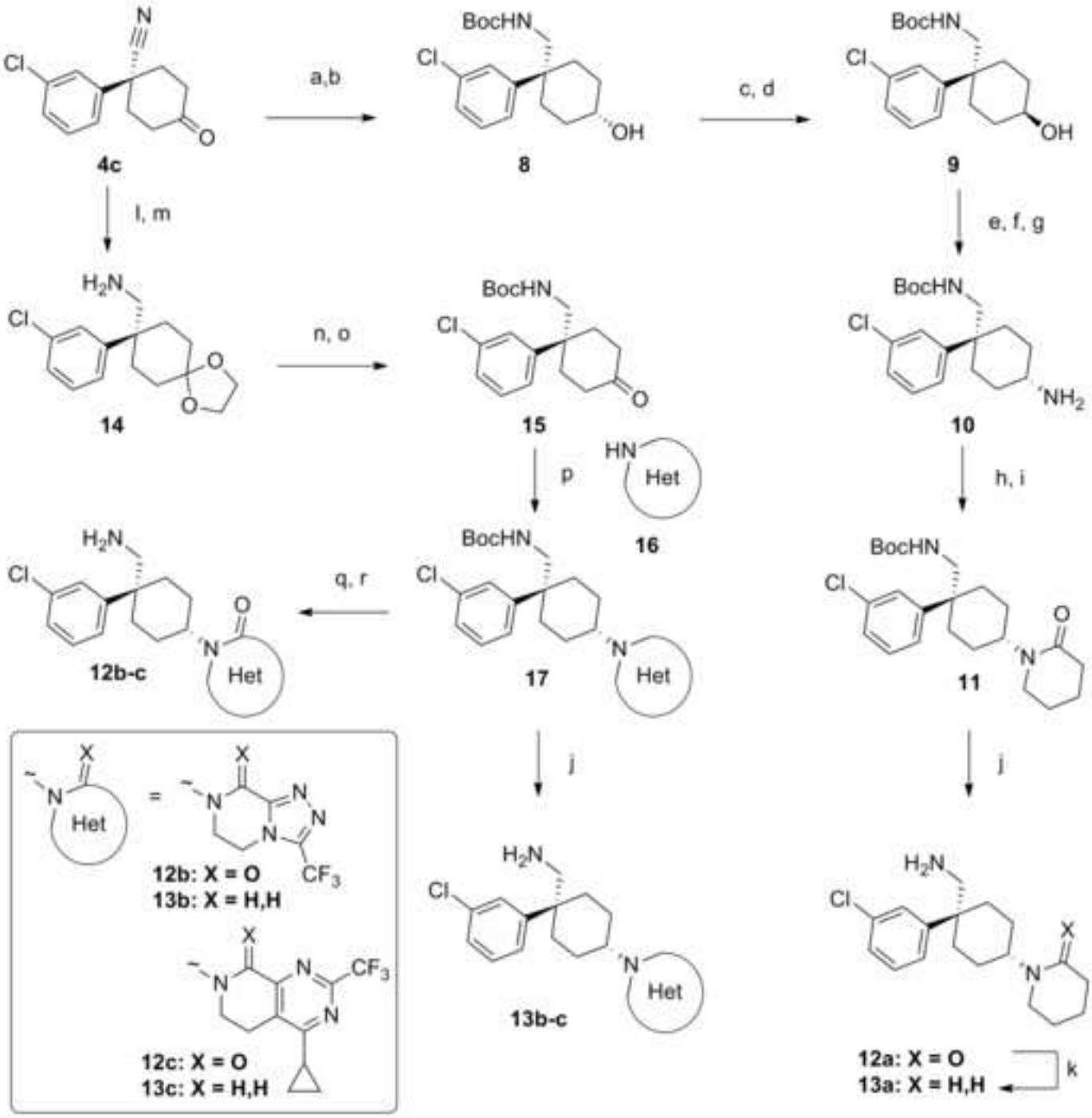

Scheme3

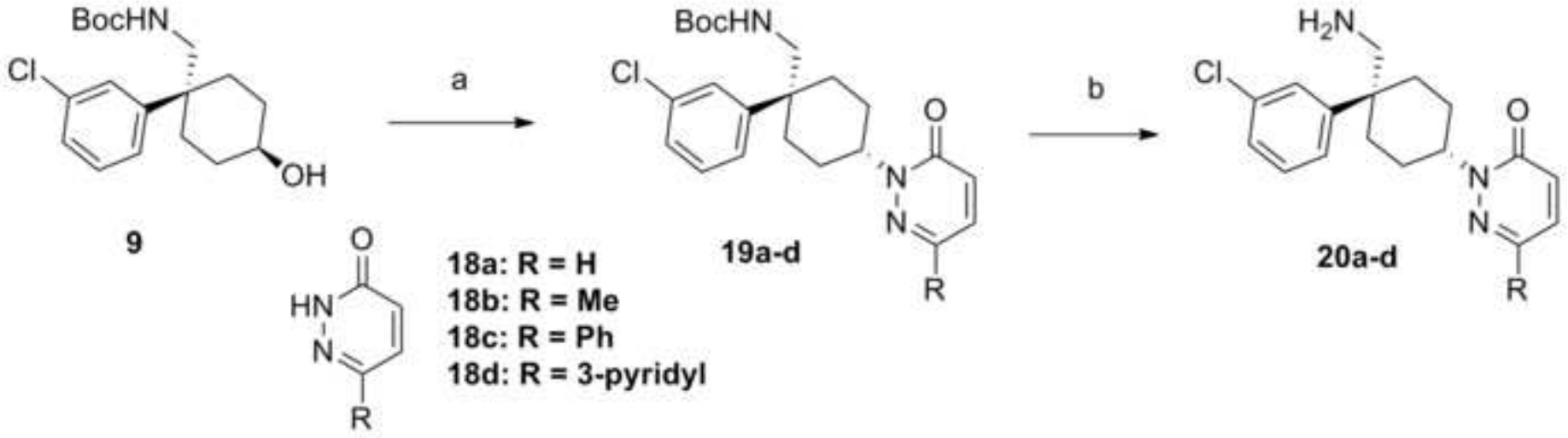

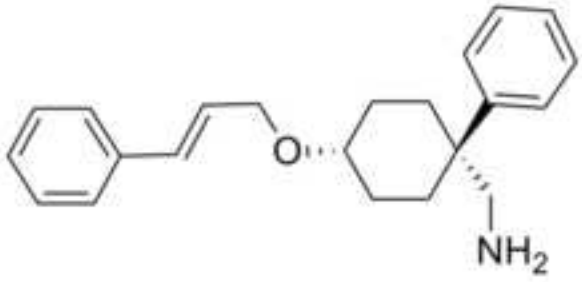

HTS hit:
***syn*-7aa**, DPP IV IC_{50} 11.9 μM

Structure-Based Drug Design

Optimal S1 binder
Water-mediated H-bond
Higher rigidity
Bicycle-biary isosterism

20d, DPP IV IC_{50} 0.004 μM;
DPP 8/9 IC_{50} >30/>30 μM;
%F(rat) 92%;
ex vivo DPP IV inhib. (rat)
>80% over 8h.